Available online at www.sciencedirect.com

SCIENCE DIRECT

Thermochimica Acta 413 (2004) 241–248

thermochimica acta

www.elsevier.com/locate/tca

Investigation of oxidation of a mineral and a synthetic engine oil

Farshid Owrang[a,*], Håkan Mattsson[a,1], Jim Olsson[b,2], Jörgen Pedersen[b,2]

[a] *Department of Reactor Physics, Chalmers University of Technology, 412 96 Göteborg, Sweden*
[b] *Arealia AB, Göteborgsvägen 91 B, SE-431 37 Mölndal, Sweden*

Received 23 September 2003; received in revised form 23 September 2003; accepted 29 September 2003

Abstract

The aim of this study was to investigate the oxidation of two different engine oils: a mineral and a synthetic engine oil. The mineral oil was a CEC[3] reference oil often used in the CEC fuel tests. The synthetic oil was biologically degradable often used for fuel tests. The oils were analyzed by liquid-state ^{13}C NMR, ^{1}H NMR and cyclic fast neutron activation analysis (cFNAA) and were oxidized at about 550 °C at atmospheric pressure in an oxidizer with constant airflow. The amount of oxygen in the condensed oil after oxidation and soot produced was measured using cFNAA. The soot produced by the mineral oil at 550 °C was studied by solid-state ^{13}C NMR.

The amount of oxygen in the mineral oil was estimated to 1.6 ± 0.2 wt.% and in the synthetic oil it was 10.1 ± 0.1 wt.%. After oxidation at 550 °C, the synthetic oil produced almost 25% more soot than the mineral oil. The amount of oxygen in the soot produced by the mineral oil was 24.9 ± 0.5 wt.% and in the soot derived by the synthetic oil it was 23.4 ± 0.5 wt.%. Seemingly, the degradation of the mineral engine oil goes via the formation of oxidized aliphatics. Interestingly, the soot derived from the mineral oil at 550 °C was similar to combustion chamber deposits (CCDs) derived from the same oil in a previous study in terms of oxygen content and chemical composition.

Keywords: Engine oil; Soot; Cyclic fast neutron activation analysis

1. Introduction

Degradation of engine oils may affect engine properties, for example through formation of combustion chamber deposits (CCDs) [1–7] and particulate emissions [8]. Engine oil is degraded due to oxidation and heat [4,9,10]. The oxidation of engine oil can be studied using several methods [3,11,12–35]. In these methods physical and chemical properties of oil during the oxidation process is studied, for example weight loss, sludge forming tendency and change in the viscosity of oil versus formation/degradation of compounds in oil. Generally, engine oil compounds have a relatively high thermal/oxidative stability [10].

Recently, we have characterized CCDs taken from a gasoline direct injection (GDI) spark ignition engine using different methods [6,7]. The engine was run with a CEC recommended reference oil [16]. The results showed that the organic part of the CCDs consisted of aliphatics (16%), oxygenated aliphatics (26%) aromatics (28%) and oxygenated aromatics, carboxyls and carbonyls (30%) [7]. There was a strong relation between the composition of the CCDs and the composition of the engine oil [7]. Seemingly, oxidation of the engine oil was an important factor for formation of CCDs in the GDI engine above. The amount of oxygen in the CCDs was between 25 and 30 wt.% depending on where the deposits were collected. Most of the oxygen was bound to compounds (acids and esters) in the volatile part of the CCDs.

The aim of this study was to investigate, using detailed methods, the oxidation of engine oils. Two different engine oils were studied: a low oxygen content mineral oil previously used in a test study of a GDI engine [5–7] and a synthetic oil containing a relatively high amount of oxygen. The oils were analyzed by liquid-state ^{13}C, ^{1}H NMR and cyclic fast neutron activation analysis (cFNAA) and were oxidized. The amount of oxygen in the condensed oil after oxidation and soot produced was measured using cF-

---

[*] Corresponding author. Tel.: +46-31-772-3085; fax: +46-31-772-3089.
E-mail addresses: farshid@nephy.chalmers.se (F. Owrang), hakan@nephy.chalmers.se (H. Mattsson), jim.olsson@arealia.com (J. Olsson).
[1] Tel.: +46-31-772-3085; fax: +46-31-772-3089.
[2] Tel.: +46-31-87-58-87; fax: +46-31-87-58-87.
[3] *CEC = Coordinating* European Council for the development of performance tests for transportation fuels, lubricants and other fluids, Brussels, Belgium [6].

0040-6031/$ – see front matter © 2003 Elsevier B.V. All rights reserved.
doi:10.1016/j.tca.2003.09.016

NAA. The soot produced by the mineral oil at 350 and 550 °C was characterized by solid-state ^{13}C NMR. This work was done as a complement to our previous study of the composition of the CCDs derived from the CEC mineral oil [7].

2. Experimental

2.1. Oils

Two different engine oils, a mineral and a synthetic oil, were analyzed in this study. Table 1 shows the property of the oils. The mineral oil was a CEC reference oil, CEC RL-189 batch 5 15W/40 SAE grade often used in the CEC fuel tests [30]. The synthetic oil was an ester based base oil containing about 15% additive.

2.2. Oxidizer

The oxidation of the oils was done in disposable sample tubes made of borosilicate ($CaB_2Si_2O_8$) with the dimensions of 12 mm × 140 mm placed on a furnace (Fig. 1). The tubes fitted precisely in the furnace part of the oxidizer. The soot produced was precipitated on the bottom of the tube and the gaseous oil out from the tube was condensed in a glass bottle by distillation. A special vent head was developed and built for air and oil introduction and gas outflow. To avoid melting of the vent head it was cooled by airflow. The angle between the experimental set-up and the floor was 15°. In this way the gaseous oil easily left the chamber.

The working temperature of the sample tubes was about 550 °C. However, the temperature varied along the tube (Fig. 2). The accuracy of the measured temperature at each point was around ±5 °C. The gas flow was adjusted to approximately 1500 ml/min using a HP Soap Film Flowmeter. At this flow, the oil vapors were rapidly transported out of the oxidizer. A graduated glass was used to measure the volume of the oils. 5 ml of each oil sample was oxidized for 25 min. The procedure was repeated four times for each type of oils.

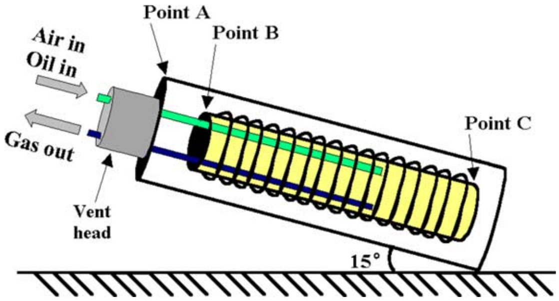

Fig. 1. Schematic figure of the oxidizer.

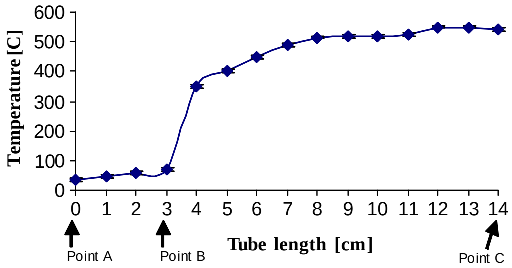

Fig. 2. Temperature along the oxidizer.

2.3. Cyclic fast neutron activation analysis

Fast neutron activation analysis is a widely used method for analysis of oxygen in a variety of matrices [7,36–38]. Oxygen can be detected by the radioactive decay of ^{16}N, produced by the nuclear reaction ^{16}O (n, p) ^{16}N. This reaction has a threshold energy of approximately 10 MeV. The ^{16}N decays with a half-life of 7.13 s, emitting 6.1 MeV (68.8%) and 7.1 MeV (4.7%) photons [39]. The sample is cyclically activated through a pneumatic transfer system. The sensitivity is good from tens of milligram up to the gram

Table 1
Specification of the engine oil

Property	Mineral oil	Synthetic oil
SAE grade	15W/40	5W/30
Density at 15 °C (g/cm^3)	0.880	0.880
Flash point (°C)	220	234
Pour point (°C)	−30	−48
Viscosity at 100 °C (cSt)[a]	14.44	12
Viscosity at 40 °C (cSt)	106.0	62
Purpose of the oil	Standard crankcase lubricant for fuel tests, gasoline and diesel	Biologically degradable, lubricant for fuel tests,
Available from	Silkolene Lubricants, Belper, Derbys UK Heinz Kruger, Oberhausen, Germany ETS, Mont-Saint-Aignan, France	Aspen Petroleum AB, Sweden

[a] 1 cSt = 10^{-6} m^2/s.

region and depends on the number of cycles and background radiation. The fast neutrons were generated by a stationary neutron generator with a neutron source strength of up to 10^{11} neutrons per second with energy of 14.1 MeV from the T (D, n) ^{4}He reaction. A BGO detector (5.08 cm × 5.08 cm) was used for detection of activated nitrogen in oils and soot. The neutron flux was monitored with a neutron detector during activation and the measured ^{16}N activity was corrected for variations in the neutron flux. The net signal is the ratio between the difference of the signal from oxygen (S_{O}) and background (S_{b}) registered by the detector and the signal from the monitor (m): $\text{Net signal} = (S_{\mathrm{O}} - S_{\mathrm{b}})/m$. The procedure and methodology of quantification of oxygen by cyclic fast neutron activation analysis (cFNAA) is described in [7]. An external standard method was used for quantification of oxygen in liquid oil and solid soot. Three calibration curves constructed by five different types of metallic powders with different volumes (and consequently weights): aluminum oxide (Al_2O_3), iron oxide (Fe_2O_3), zinc oxide (ZnO), sodium bicarbonate ($NaHCO_3$) and calcium oxide (CaO).

2.4. Liquid-state ^{13}C and ^{1}H NMR

For comparing the chemical composition of engine oils, the oils were analyzed by liquid-state ^{13}C and ^{1}H NMR (nuclear magnetic resonance) spectroscopy. NMR is a powerful method for investigation of the composition of different types of oil NMR [40–43]. ^{13}C NMR was run unlocked without any deuterated solvent. TMS was used as internal reference and no relaxation agent was used. ^{13}C NMR was recorded qualitative with a 90° pulse and the time between the pulses was 15 s. All the spectra were recorded at 25 °C on a Varian Inova 600 MHz spectrometer equipped with a bb-probe (5 mm NMR tube with 700 μl sample volume). The ^{1}H NMR was performed on a Varian Inova 500 spectrometer at resonance frequencies 125.672 and 499.746 MHz. The probe used for accumulating the ^{1}H data was a Varian PFG probe. The recycle delay was 1 s and no proton-decoupling field was used.

2.5. Solid-state ^{13}C NMR

In the present study, a single pulse ^{13}C solid-state NMR was used to characterize the organic compounds in the soot derived from the mineral oil. Solid-state ^{13}C NMR spectroscopy was performed on a Varian Inova 500 MHz spectrometer with magic angle spinning. The resonance frequency for ^{13}C was 125.673 ppm and the recycle delay was 1 s. No proton decoupling was used. The probe used was a room temperature CP/MAS probe. The samples were ground and homogenized. Around 100 mg was packed into a 5 mm rotor. The ferromagnetic impurities were removed using a bar magnet. The run time for each sample was 45 min with the spinning rate of 8000 Hz. At this spinning rate the spinning side band is minimized. In this method, carbon atoms in different compounds were monitored at different chemical shift ranges. Chemical shifts of hexamethylbenzene ($C_{12}H_{18}$) were used for referencing the spectra. The relative amount of every type of compound was calculated using integration of the area under the peak. To identify the chemical shift of the compounds contained in the mineral engine oil, 100 μl unused engine oil was run in the rotor with magic angle spinning. The spinning rate of this sample was 600 Hz.

3. Results and discussions

3.1. Liquid-state ^{13}C and ^{1}H NMR of oils

The results from the liquid-state ^{13}C NMR (Fig. 3a and b) and ^{1}H NMR (Fig. 4a and b) give information about the chemical composition of the mineral oil and the synthetic oil, respectively. In these spectra, each peak corresponds to a specific functional group; the area under the peak is proportional to the concentration of the compound. The relevant peaks were verified using a database [44] and compared to the results in Ref. [45]. The chemical shift from 60 to 0 ppm in Fig. 3a and b corresponds to the different aliphatic (alkyl-) functional groups. As seen in Fig. 3a, the mineral oil contains only aliphatics. Fig. 3b shows that the synthetic oil has in addition to the aliphatic peaks, two peaks at 171

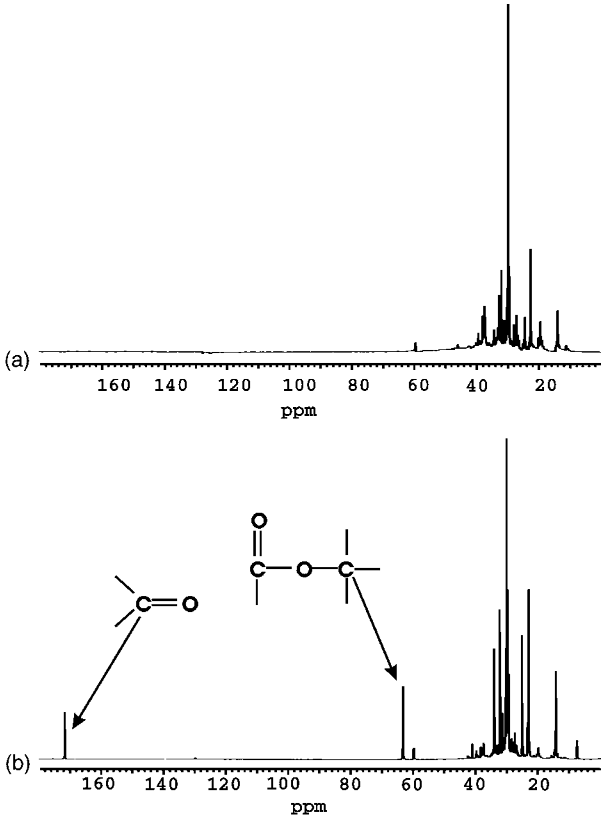

Fig. 3. (a) Liquid-state ^{13}C NMR of the mineral oil; (b) liquid-state ^{13}C NMR of the synthetic oil.

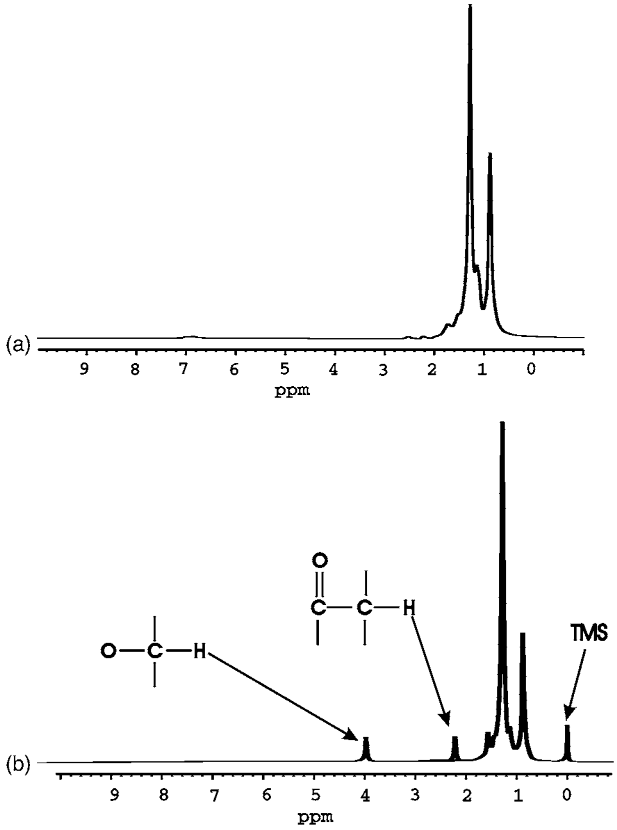

Fig. 4. (a) Liquid-state ^{1}H NMR of the mineral oil; (b) liquid-state ^{1}H NMR of the synthetic oil.

and 63 ppm, respectively (marked by labels in Fig. 3b). The peak at 171 ppm corresponds to carbon of the carbonyl group (C=O) and the peak at 63 ppm refers to carbon of an ester group (C–O–C). The ^{1}H NMR of the mineral oil in Fig. 4a and b shows two peaks in the chemical region 1.8–0 ppm corresponding to aliphatic (alkane) functional groups. As seen in Fig. 4a, the mineral oil consists of aliphatics. The peak between 2.0 and 1.0 ppm corresponds to methyl protons [45]. The peak at 2.1 ppm in Fig. 3b corresponds to hydrogen of a methyl group bound to a carbonyl group and the peak at 3.9 ppm refers to hydrogen of a methyl group bound to an ester group.

3.2. Gravimetric analysis of soot

Gravimetric analysis of soot, produced from the oils investigated, was done using a precision balance (E. Mettler Cap. 80 g). The results are given in Tables 2 and 3. The oxidation procedure generated very reproducible results. This is evident from the low values of standard deviation in Table 3. This table shows that the amount of soot derived from the 5 ml (4.4 g) mineral oil is about 3.7 wt.% and from the 5 ml (4.4 g) synthetic oil it is about 4.6 wt.%. The synthetic oil produced approximately 25% more soot than the mineral oil.

As a test, the temperature of the oxidizer was changed to 350 °C and the sludge left in the sample tube after 25 min produced by oxidation of the mineral oil was weighed. 5 ml mineral oil produced 1.166 g sludge. The sludge was a black mixture consisting of unburned and burned engine oil and soot fragments.

Table 2
The amount of soot produced from the oils at different procedures

Procedure	Soot [g] from mineral oil	Soot [g] from synthetic oil
1	0.16291	0.20080
2	0.16311	0.20161
3	0.16202	0.20211
4	0.16270	0.19891

3.3. Cyclic fast neutron activation analysis (cFNAA) of oils and soot

The mineral oils, the condensed oils, and the soot were measured at three different times with slightly different experimental set-up. Fig. 5a–c show three different calibration curves, from the three different cFNAA experiments, made of different metal oxide powders. Note that for activation analysis the type of powder is not important, as the neutron attenuation in the powder samples is almost the same. Fig. 5a shows a calibration curve made with aluminum oxide and iron oxide used for quantitative analysis of oxygen in the mineral oil and the synthetic oil. This curve was previously used for quantification of oxygen in CCDs [7]. The dimension of the container for standards was 14 mm × 32 mm and for oils it was 15 mm × 54 mm. Generally, for liquid samples, the sample containers were sealed carefully by melting the cap to the container. The number of cycles was 6.

As seen in Fig. 5a the amount of oxygen depends linearly on the activity corrected for variation in neutron flux. Metallic elements (zinc, phosphorus, calcium and magnesium potassium) and sulfur exist in much smaller amounts than oxygen in the oil and do not interfere with oxygen at all.

Fig. 5b shows a calibration curve made with the ZnO and $NaHCO_3$ used for determination of oxygen in the condensed mineral oil and condensed synthetic oil. The dimension of the container for powder standards and liquid oil samples was 15 mm × 54 mm. The number of cycles was 12, which is an increase by a factor 2 compared to the calibration curve in Fig 5a. Theoretically, this would decrease the statistical errors in the net signal by a factor of $1/\sqrt{2}$, which can give a more accurate calibration curve. The linear relation between the measurement points in Fig. 5b indicates that

Table 3
The average amount of soot produced from the oils

Oil	Soot [g] (average)	S.D.	% soot 5 ml sample
Mineral oil	0.1627	0.0006	3.7
Synthetic oil	0.2009	0.0014	4.6

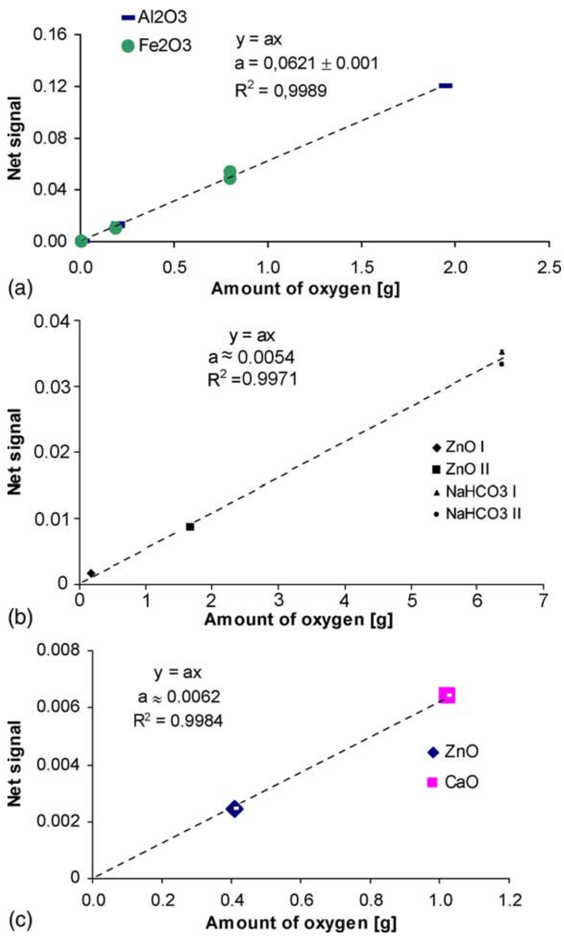

Fig. 5. (a) cFNAA calibration curve with Al_2O_3 and Fe_2O_3 (values in Table 4); (b) cFNAA calibration curve with ZnO and $NaHCO_3$ (values in Table 5); (c) cFNAA calibration curve with ZnO and CaO (values in Table 6).

fewer standard samples can also give a curve with good accuracy.

Fig. 5c shows a calibration curve made with the ZnO and CaO used for determination of oxygen in the soot derived from the mineral oil and synthetic oil. The dimension of the container for powder standards and powder soot samples was 14 mm × 32 mm. Because the amount of soot was small, the number of cycles was increased to 18. Theoretically, this would decrease the statistical errors in the net signal by a factor of $1/\sqrt{3}$. The correlation factor (R^2) of the curve is very low (0.9984). The low error in the curve in Fig. 5c indicates that only two standards can give a good estimation of oxygen in the soot and the sludge samples.

Tables 4–6 show the amount of oxygen in the engine oils, condensed engine oils after oxidation, and soot produced using the calibration curve shown in Fig. 4. According to Fig. 5a and Table 4, there is 0.103 ± 0.003 g oxygen in 6.690 g mineral oil (1.6 ± 0.2 wt.%). In the synthetic oil the amount of oxygen was 0.65 ± 0.01 g in 6.48 g oil (10.1 ± 0.1 wt.%). The synthetic oil contains about six times more oxygen than the mineral oil.

Table 4
Data for cFNAA of the mineral and synthetic oil (graphic plot in Fig. 5a)

Standard	Amount of oxygen [g]	Net signal	Statistical errors, net signal
Fe_2O_3	0.006	0.0006	0.0001
Al_2O_3	0.014	0.0005	0.0001
Al_2O_3	0.014	0.0007	0.0001
Fe_2O_3	0.188	0.0106	0.0002
Al_2O_3	0.200	0.0122	0.0002
Al_2O_3	0.200	0.0138	0.0002
Fe_2O_3	0.799	0.0490	0.0003
Fe_2O_3	0.799	0.0539	0.0003
Al_2O_3	1.946	0.1201	0.0005
Al_2O_3	1.946	0.1208	0.0006
Sample	Weight sample [g]		
Mineral oil	6.690	0.0064	0.0010
Synthetic oil	6.480	0.0406	0.0003

Table 5
Data for cFNAA of oils and condensed oils after oxidation (graphic plot in Fig. 5b)

	Amount of oxygen [g]	Net signal	Statistical errors, net signal
ZnO I	0.171	0.0016	0.0000
ZnO II	1.680	0.0086	0.0001
$NaHCO_3$ I	6.375	0.0352	0.0002
$NaHCO_3$ II	6.375	0.0333	0.0002
Sample	Weight sample [g]		
Condensed mineral oil	7.290	0.0022	0.0000
Condensed synthetic oil	7.079	0.0058	0.0001

According to Fig. 5b and Table 5, the amount of oxygen in the condensed mineral oil was about 0.407 g oxygen in 7.290 g oil (5.6 wt.%) and in the condensed synthetic oil it was 1.074 ± 0.019 g in 7.079 g oil (15.1 ± 0.3 wt.%). After oxidation, the synthetic oil contains about 2.7 times more oxygen than the mineral oil.

From each oil sample, the four soot samples derived were mixed and analyzed with cFNAA. According to Fig. 5c and Table 6, the amount of oxygen in the soot derived from the mineral oil was 0.273 ± 0.006 g in 1.095 g soot (24.9 ± 0.5 wt.%) and in the synthetic oil it was 0.272 ± 0.006 g

Table 6
Data for cFNAA of soot and sludge (graphic plot in Fig. 5c)

Standard	Amount of oxygen [g]	Net signal	Statistical errors, net signal
ZnO	0.408	0.0024	0.00001
CaO	1.025	0.0064	0.00010
Sample	Weight sample [g]		
Soot, mineral oil	1.095	0.00169	0.00004
Soot, synthetic oil	1.167	0.00169	0.00004
Sludge	1.166	0.00070	0.00010

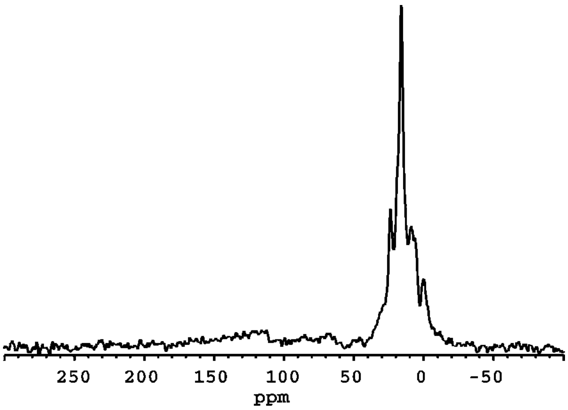

Fig. 6. ^{13}C NMR of the mineral engine oil analyzed using the CP/MAS probe.

in 1.167 g oil (23.4 ± 0.5 wt.%). This indicates that soot produced by the mineral oil is ca 9% more oxidized than soot derived from the synthetic oil. Using the calibration curve in Fig. 5c the amount of the oxygen in the sludge produced at 350 °C derived from the mineral oil was estimated to 0.113 ± 0.016 g in the 1.166 g sludge (9.7 ± 1.4 wt.%).

3.4. *Solid-state ^{13}C NMR of soot*

Fig. 6 shows ^{13}C NMR of the mineral engine oil analysed using the CP/MAS probe. In this figure, aliphatics contained in the mineral engine oil are presented by a broad peak in the region 40–0 ppm.

Fig. 7 shows solid-state ^{13}C NMR of the sludge produced at 350 °C (Section 3.2). The major fraction of the sludge consists of unburned engine oil in the region 40–0 ppm. The small but broad peak in the region 60–40 ppm comes from oxygenated aliphatic functional groups indicating that oxygenated aliphatics form at lower temperature.

Fig. 8 shows the ^{13}C solid-state NMR of the soot derived from the mineral oil at 550 °C. Table 6 shows area fractions of important chemical shift regions in the NMR spectrum in Fig. 8. As seen in this table, a significant part of the soot (40–0 ppm) consists of unburned engine oil. Compounds containing oxygen (oxygenated aliphatics and carboxyls and carbonyls) make up for almost 50% of the deposits. Interestingly, the soot derived from the mineral oil is very similar to CCDs analysed in [7] in terms of oxygen content and chemical composition (Table 7).

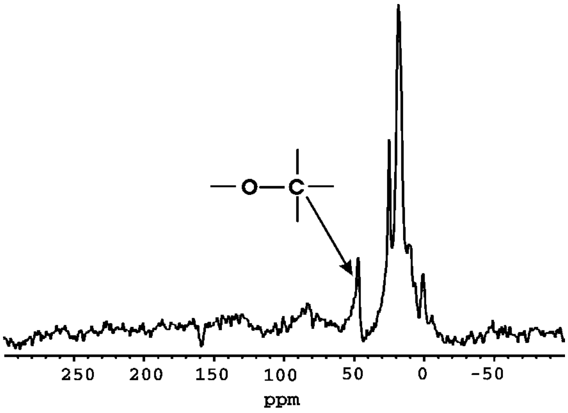

Fig. 7. Solid-state ^{13}C NMR of the sludge derived from the mineral oil at 350 °C.

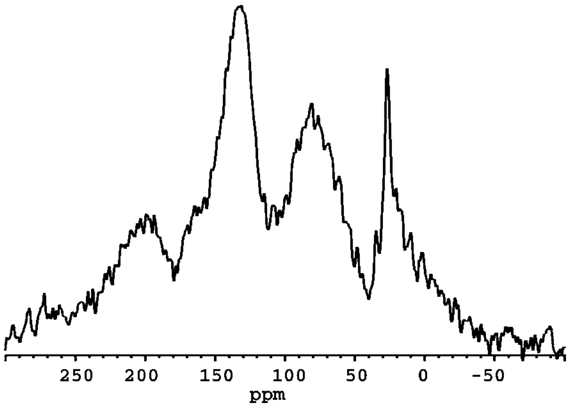

Fig. 8. Solid-state ^{13}C NMR of the soot derived from the mineral oil at 550 °C.

Table 7
Approximate area fraction of important chemical shift regions in the NMR spectra of soot derived from the mineral oil at 550 °C

Compound classes	Chemical Shift (ppm)	Area fraction (%)
Aliphatics	40–0	16
Oxygenated aliphatics	110–40	29
Aromatics	160–110	31
Oxygenated aromatics	180–160	8
Carboxyls and carbonyls	250–180	16

The future work may focus on the characterization of oxidized oil and sludge/soot produced from the mineral oil at different conditions: temperature, pressure and airflow by fast cFNAA with more than 18 cycles and high resolution (cross-polarization) solid-state NMR spectroscopy.

4. Conclusion

The amount of oxygen in the mineral oil was estimated to 1.6±0.2 wt.% and in the synthetic oil it was 10.1±0.1 wt.%. After oxidation at 550 °C, the synthetic oil produced almost 25% more soot than the mineral oil. The amount of oxygen in the soot produced by the mineral oil was 24.9±0.5 wt.% and in the soot derived by the synthetic oil it was 23.4±0.5 wt.%. Seemingly, the degradation of the mineral engine oil goes via the formation of oxidized aliphatics. Interestingly, the soot derived from the mineral oil at 550 °C was similar to combustion chamber deposits (CCDs) derived from the same oil in a previous study in terms of oxygen content and chemical composition.

Acknowledgements

The authors gratefully acknowledge the technical support provided by the Messrs. L. Norberg and L. Urholm of the Department of Reactor Physics. Special thanks go to Dr. Anders Nordlund for valuable theoretical support to this work.

References

[1] L.B. Ebert, Chemistry of Engine Combustion Chamber Deposits, Plenum Press, New York, 1985, ISBN 0-306-41936-X.

[2] L.B. Ebert, W.H. Davis, D.R. Mills, D.I. Dannerlein, D.L. Rose, M.T. Melchior, The chemistry of internal combustion engine deposits. Parts, I, II and III of [1].

[3] J.C. Wang, M.A. Sublette, High temperature liquid lubricant development. Part I. Engine tests, SAE Technical Paper Series, SAE 932842, 1993.

[4] J.S. Kim, B.S. Min, D.S. Lee, D.Y. Oh, J.K.. Choi, The characteristics of carbon deposit formation in piston top ring groove of gasoline and diesel engine, SAE Technical Paper Series, SAE 980526, 1998.

[5] H. Sandquist, Emission and Deposit Formation in Direct Injection Stratified Charge SI Engine. Thesis, Chalmers University of Technology, ISBN 91-7291-075-5 (2001).

[6] H. Sandquist, I. Denbratt, F. Owrang, J. Olsson, Influence of fuel parameters on deposit formation and emissions in a direct injection stratified charge SI engine, SAE Technical Paper Series, SAE 2001-01-05, 2001.

[7] F. Owrang, H. Mattsson, A. Nordlund, J. Olsson, J. Pedersen, Characterization of combustion chamber deposits from a gasoline direct injection SI engine, SAE technical paper, SAE 2003-01-0546, 2003.

[8] G. Tondelli, M. Carriero, A. Pedicillo, Combustion chamber deposits: fuel and lubricant effects on exhaust hydrocarbon emissions measured by fast FID analyser, SAE Technical Paper Series, SAE 2000-01-2024, 2000.

[9] J.L. Lauer, P.J. Friel, Some properties of carbonaceous deposits accumulated in internal combustion engines, Combust. Flame 4 (1960) 107.

[10] R.M. Mortier, S.T. Orszulik, Chemistry and Technology of Lubricants, second edition, Edmundsbury Press, Suffolk, 1997, pp. 98–144, ISBN: 0-7514-0246-X.

[11] K.A. Egorova, B.S. Zuseva, V.A. Filimontseva, A.N. Zeitseva, Investigation of oxidation stability of certain mineral oils by means of infrared spectroscopy, Chem. Technol. Fuels Oils 12 (1970) 790.

[12] F. Noel, Thermal analysis of lubricating oils, Thermochimica. Acta 4 (1972) 377.

[13] K.A. Egorova, B.S. Zuseva, V.A. Filimontseva, A.N. Zeitseva, Chem. Technol. Fuels Oils 12 (9–10) (1976) 790.

[14] H.A. Naga, A.E.M. Salem, Base oils thermooxidation, Lubricat. Eng. 42 (1986) 210.

[15] H.A. Naga, A.E.M. Salem, Testing the thermooxidation of lubricating oils via differential thermal analysis, J. Thermal Anal. 32 (1987) 1401.

[16] J.E. Davis, Oxidation characteristics of some engine oil formulations containing petroleum and synthetic basestocks, Lubricat. Eng. 43 (1987) 199.

[17] H.A. Naga, A.E.M. Salem, The effect of base stock volatility on lubricating oil oxidation stability, Lubricat. Eng. 44 (1987) 931.

[18] A. Sasaki, M. Kawasaki, T. Sakai, H. Kojirna, S. Takayama, The use of electrostatic liquid for contamination control of hydraulic oil, Lubricat. Eng. 44 (1988) 251.

[19] A. Sasaki, M. Kawasaki, T. Sakai, H. Kojirna, S. Takayama, A study of hydraulic valve problems, Lubricat. Eng. 45 (1989) 140.

[20] A. Sasaki, T. Tobisu, S. Uchiyama, T. Sakai, M. Kawasaki, Uchiyama, evaluation of molecular weight and solubility in oil of the oxidation products of two different types of oils, Lubricat. Eng. 47 (1990) 809.

[21] B. Latto, J. Yang, Thermo-oxidation Effect on Viscosity of 10W30 Oil with XM-5 or STP, Lubricat. Eng. 47 (1991) 455.

[22] D.W. Florkowski, T.H. Selby, The development of a thermo-oxidation engine oil simulation test (TEOST), SAE Technical Paper Series, SAE 932837, 1993.

[23] W.K. Cheng, S. Hochgreb, M.G. Norris, K. Wu, Auto-oil program phase II heavy hydrocarbon study: fuel species oxidation chemistry and its relationship to the auto-oil data, SAE Technical Paper Series, SAE 941970 (1994).

[24] A. Zeman, A. Sprengel, D. Niedermeier, M. Späth, Biodegradable lubricants—studies on thermo-oxidation of metal-working and hydraulic fluids by differential scanning calorimetry (DSC), Thermochim. Acta 268 (1995) 9.

[25] A.J. Stipanovic, J.P Schoonmaker, E.F. de Paz, J.K. Mowlem, J.E. Broas, C.Y. Thiel, Base oil and additive effects in thermo-oxidation engine oil simulation test (TEOST), SAE Technical Paper Series, SAE 962038, 1996.

[26] D. Faure, J.C. Hipeaux, Y. Guevellou, A. Legros, Oxidation stability of gasoline engine lubricants: effect of base oil chemistry in different laboratory and engine tests, CEC Technical Paper Series, CEC97-EL03, 1997.

[27] M.A.M. El-Qurashi, H.M. Ali, Anilinosilanes as thermo-oxidation stabilizers of commercial lubricating base oils, Thermochim. Acta 293 (1–2) (1997) 185.

[28] G. McCullough, R. Douglas, A.P.N. McDowell, R.G. Kenny, An experimental evaluation of the oil fouling effects of two-stroke oxidation catalysts, SAE Technical Paper Series, SAE 982014, 1998.

[29] A. Adhvaryu, Y.K. Sharma, I.D. Singh, Studies on the oxidative behavior of base oils and their chromatographic fractions, Fuel 78 (1999) 1293.

[30] K. Daniel, T.J. Aarnink, M. Gairing, H. Schmidt, Combustion chamber deposits and their evaluation by a european performance test, SAE Technical Paper Series, SAE 2000-01-2023, 2000.

[31] J. Cerny, Z. Strnad, Z.G. Sebor, Composition and oxidation stability of SAE 15W-40 engine oils, Tribol. Int. 34 (2001) 127.

[32] A. Adhvaryu, S.Z. Erhan, S.K. Sahoo, I.D. Singh, Thermo-oxidative stability studies on some new generation API group II and III base oils, Fuel 81 (2002) 785.

[33] B.N. Barman, Behavioral differences between group I and group II base oils during thermo-oxidative degradation, Tribol. Int. 35 (2002) 15.

[34] C.D. Gamlin, N.K. Dutta, N.R. Choudhury, D. Kehoe, J. Matisons, Evaluation of kinetic parameters of thermal and oxidative decomposition of base oils by conventional, isothermal and modulated TGA, and pressure DSC, Thermochim. Acta 392 (2002) 357.

[35] B.K. Sharma, A.J. Stipanovic, Development of a new oxidation stability test method for lubricating oils using high-pressure differential scanning calorimetry, Thermochim. Acta 402 (2003) 1.

[36] K. Randle, Applications of fast neutron activation analysis (FNAA) at Birmingham, Nucl. Measure. Methods Phys. Res. B 24/25 (1987) 1010.

[37] S.S. Nargolwalla, E.P. Przybylowicz, Activation Analysis with Neutron Generators, Wiley, New York, 1973, ISBN 0-471-63031-4.

[38] D. De Soete, R. Gijbels, J. Hoste, Neutron Activation Analysis. Wiley-Interscience, ISBN 0-471-20390-4 (1972).

[39] J.W. McKlveen, Fast Neutron Activation Analysis Elemental Data Base, Ann Arbor Science, Ann Arbor, MI, 1981, ISBN: 0-250-40406-0.

[40] M.B. Smirnov, E.B. Frolov, A study of petroleum alkylcarbazoles using ^{1}H NMR spectroscopy, Org. Geochem. 26 (1997) 33.

[41] M.M. Maroto-Valer, J.M. Andrésen, C.E. Snape, Quantification by in situ ^{1}H NMR of the contributions from pyridine-extractables and metaplast to the generation of coal plasticity, Fuel 76 (1997) 1301.

[42] A. Rafenomanantsoa, D. Nicole, P. Rubini, J.C. Lauer, NMR and FIMS structural analysis of the oil obtained from the pyrolysis of Bemolanga tar-sand bitumen (Madagascar) according to a post combustion process, Fuel 77 (1998) 33.

[43] D.A. Netzel, J.P. Turner, ^{1}H NMR study of the hydration kinetics of coal fly ash and spent oil shale, Fuel 80 (2001) 303.

[44] SDBS Integrated Spectral Data Base System for Organic Compounds, SDBSWeb: http://www.aist.go.jp/RIODB/SDBS/ (access date (2001).

[45] M.A. Khan, I. Ahmad, M. Ishaq, M. Shakirullah, M.T. Jan, E. Rehman, A. Bahader, Spectral Characterization of Liquefied Products of Pakistani Coal, Fuel Processing Technology 85 (2003) 63.